Rare Metal Materials and Engineering
Volume.50, Issue.4, April 2021
Available online at **www.rmme.ac.cn**

Science Press

Cite this article as: Xu Rongfu,Li Changhou,Xu Yong,et al.Centrifugal Investment Casting of Ti-47Al-6Nb Exhaust Valves[J].Rare Metal Materials and Engineering,2021,50(04):1173-1178.

Centrifugal Investment Casting of Ti-47Al-6Nb Exhaust Valves

Xu Rongfu, Li Changhou, Xu Yong, Zhang Dongming, Shi Yueya

School of Materials Science and Engineering, Shandong Jianzhu University, Jinan 250101, China

Abstract: The shell mold filling process for high-Nb TiAl alloy exhaust valve casting prepared by centrifugal investment casting was investigated. Composition of the casting and shell mold was Ti-47Al-6Nb (at%) and zircon sand, respectively. As a comparison and verification of the simulation results, a series of shell mold filling experiments of centrifugal casting were carried out. Simulation results indicate that the shell mold filling time is about 3.8 s; casting defects are distributed along the central line of the exhaust valves, especially in the neck position. The comparison shows that the simulation results agree with experiments. The powder/liquid ratio of 1.5∶1 and mixing time of 30 min are identified as the proper process for the inner layer slurry in the process of making shell mold. There are no noticeable interfacial reactions between casting and shell mold according to XRD analysis. The metallurgical analysis results reveal that the lamellar structure is the typical structure of the as-cast exhaust valves, with a grain size of 185~300 μm.

Key words: exhaust valves; numerical simulation; macroscopic defects; microstructure

Nowadays, the ultra-lightweight alloys and the environmental pollution of the tail gas of motor vehicles have become the focus in the modern car industry. Exhaust valve, as one of the most critical parts of the automotive engine, has been a particular focus of the drive for improving engine performance or achieving the purpose of energy-saving and emission reduction. To improve the engine's efficiency and reduce pollutant emissions, the substitution of ultra-lightweight materials for steel is a practical approach. However, exhaust valves are subjected to long-term exposure to high temperature (600~900 °C) and corrosive gas environment. Therefore, the exhaust valve material should have excellent heat resistance and high-temperature corrosion resistance. Based on these facts, conventional lightweight materials cannot meet the working conditions for exhaust valves[1, 2]. At present, TiAl based intermetallic alloy appears to be an ideal candidate material for the exhaust valves due to its low density (3.8 g/cm^3), high specific strength, high Young's modulus, creep resistance and oxidation resistance at elevated temperatures[3, 4]. Moreover, the addition of element niobium (Nb) can also improve the service temperature up to 800 °C and enhance the oxidation resistance at high temperatures[5, 6]. There are some advantages for the application of TiAl alloy exhaust valves in automotive engines, such as improving engine performance, energy-saving, emission reduction, and more environment-friendly, expanding the engine application range.

Although TiAl alloy has many advantages as mentioned above, it also has some shortcomings. Characteristics of TiAl alloy are as follows: high brittle-ductile transition temperature, narrow solidification range, poor deformability, etc[7-9]. Up to now, there are three methods to shape TiAl alloy parts: casting, powder metallurgy (PM), and forging. Due to inherent shortcomings, it is challenging to process TiAl alloy by forging[10]. Besides, the difficulty in the preparation of TiAl alloy powder restricts the application of powder metallurgy. In contrast, investment casting, which has advantages of low cost and net shape, has great potential in large-scale production of TiAl alloy exhaust valves. To improve the flow rate of alloy melt and to enhance the fluidity of the TiAl alloy, the centrifugal casting process is particularly effective[11]. In short, the precision casting process and parameters are prerequisites to get the best quality casting of TiAl alloy. With the development of computer technology, the numerical simulation technique shows good advantages over the conventional trial-and-error methodologies for casting process design and optimization. During the production of TiAl castings, the use of numerical

Received date: April 22, 2020
Foundation item: Doctoral Scientific Fund Project of Shandong Jianzhu University (XNBS1430)
Corresponding author: Xu Rongfu, Ph. D., Lecturer, School of Materials Science and Engineering, Shandong Jianzhu University, Jinan 250101, P. R. China, Tel: 0086-531-86367286, E-mail: 13559@sdjzu.edu.cn

simulation can reduce the production cost and shorten the production cycle. The engineers must know the metallurgical capabilities of the casting process used early. In conclusion, casting process simulation and optimization based on a numerical method have been widely used in precision casting.

The purpose of this research is to simulate the shell mold filling process of high-Nb TiAl exhaust valves. The actual pouring experiment was carried out to verify the casting process and the shell mold making process. The casting defects, XRD analysis, and microstructures of TiAl exhaust valves were also adopted to investigate the possibility of the centrifugal investment casting process for the mass production of high-Nb TiAl exhaust valves.

1 Experiment

The finite element software was used to simulate the shell mold filling process and predict the shrinkage/porosity defects during solidification. Composition of the casting and shell mold was Ti-47Al-6Nb (at%) and zircon sand, respectively. The thermophysical properties of the used TiAl alloy and shell mold materials are listed in Table 1. The initial processing parameters used in the simulation are as follows: pouring temperature, 1700 °C; filling time, 5 s; pre-heated shell mold temperature, 20 °C; interface heat transfer coefficient, 500 $W \cdot m^{-2} \cdot K^{-1}$; centrifugal rotation speed, 300 r/min.

The schematic illustration of the exhaust valve, as shown in Fig.1a, has a total length of about 60 mm, with the head diameter of Φ40 mm and the stem with the dimension of Φ9 mm×50 mm. To meet the requirement of the subsequent actual pouring experiment, a "tree-type" of an optimized three-dimensional (3D) gating system is used, as shown in Fig. 1b. Due to the centrifugal force and solidification, eight parts with the horizontal arrangement were placed on the tree in regular distribution. Cast parameters used in the experiments were the same as those in the simulation, as described above.

To ensure the shell mold surface quality, it is cautioned that the shell should be dried before the next coating layer was brushed, and drying time should be extended before shell mold was dewaxed. The primary coating of the inner shell, also referred to as the first two coating layers, determines the surface quality of the castings. In the present work, the ZrO_2-flour-zirconium sol slurry was used as colloidal suspension and ZrO_2 power. Secondary coating, referred to as the third to seventh coating layers, was made of the slurry of zirconia sol and covered with ZrO_2 power (particle size ranging from 200 μm to 500 μm). The total thickness of the shell mold was approximately 8 mm. After the fabricated shell mold was completely dried, it was dewaxed and sintered at different temperatures to obtain the ceramic shell mold with high-temperature strength. The sintered process curve for the shell mold is shown in Fig.2. The physical images of the shell mold at different stages are shown in Fig.3.

Table 1 Thermophysical properties of TiAl alloy and shell mold materials

	Parameter	Value
Ti-47Al-6Nb	Conductivity/$W \cdot m^{-1} \cdot K^{-1}$	15-26
	Density/$kg \cdot m^{-3}$	4135~4513
	Specific heat/$kJ \cdot kg^{-1} \cdot K^{-1}$	0.63~1.02
	Enthalpy/$kJ \cdot kg^{-1}$	330
	Liquidus/°C	1578
	Solidus/°C	1405
	Viscosity/$\times 10^{-3}$ Pa·s	4.65~8.8
Ceramic mold	Conductivity/$W \cdot m^{-1} \cdot K^{-1}$	0.83~0.97
	Density/$kg \cdot m^{-3}$	2780
	Specific heat/$kJ \cdot kg^{-1} \cdot K^{-1}$	0.44~0.85

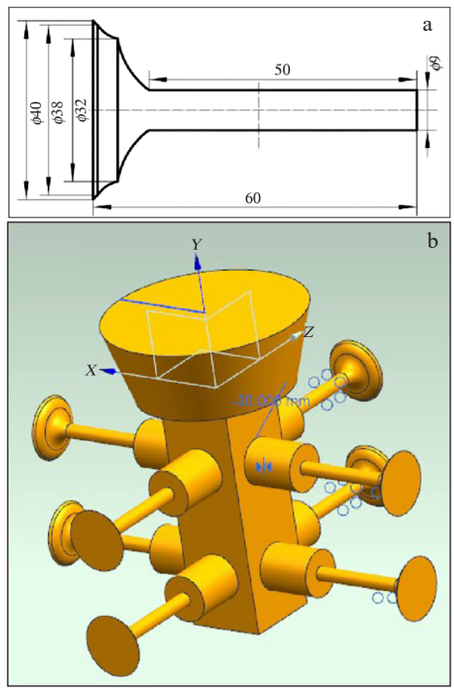

Fig.1 Schematic illustration of the exhaust valve (a) and 3D model of the gating system (b)

In the actual experiment, Ti-47Al-6Nb (at%) alloy was melted by induction skull melting (ISM) process. The two-step melting process for the alloy was adopted to obtain the uniform composition of cast ingot. In the second remelting for ingot, the centrifugal casting process was adopted to shape the castings. In other words, when the temperature of the molten alloy and rotation speed of the ceramic shell mold were adjusted to the pre-determined parameters, the melt was directly poured into the turning shell mold to shape the casting.

To inspect defects in exhaust valves, the specimen was sectioned along the center axis of the stem for valves. According to the specimen cutting diagram, as shown in Fig.4, a series of metallographic specimen (specimens 1, 2, 3, 4) were sectioned and prepared by electro-polishing for TiAl alloys. The microstructures were characterized by the optical microscope (OM). The phase structure was detected by X-ray diffraction (XRD, BRUKER D8 ADVANCE), operated at 40 kV

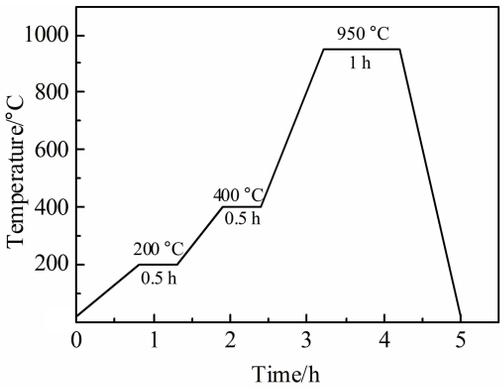

Fig.2 Sintering process curve of the shell mold

and 40 mA with Cu Kα. The Kroll's reagent (5vol% HF, 10vol% HNO_3, and 85vol% H_2O) was used.

2 Results and Discussion

2.1 Processing simulation and actual casting

Based on the initial processing parameters as described above, the simulation of temperature field, flow field, and pressure field of the centrifugal casting process for exhaust valves made of TiAl based alloys was performed. The typical simulation results for the shell mold filling process for exhaust valves are shown in Fig.5. It is revealed that the molten alloy flows along with the suction of the shell and is poured into the cavity under the centrifugal force. The shell mold filling time is about 3.8 s. After 3.89 s (as shown in Fig. 5d), the shell mold

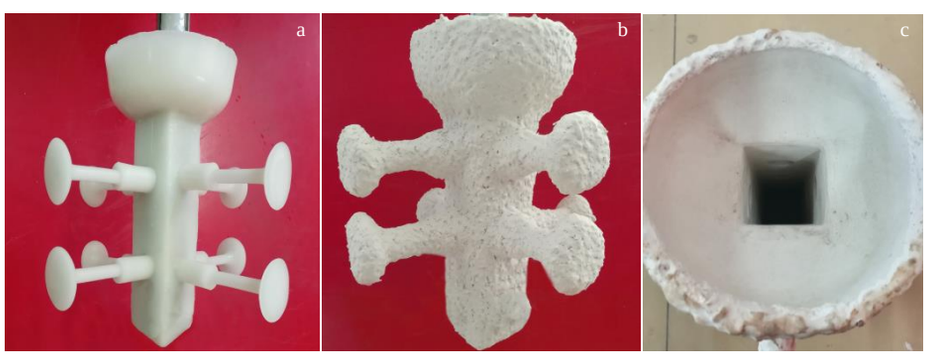

Fig.3 Physical images of the assembled wax mold (a), the cured shell mold (b) and the sintered shell mold (c)

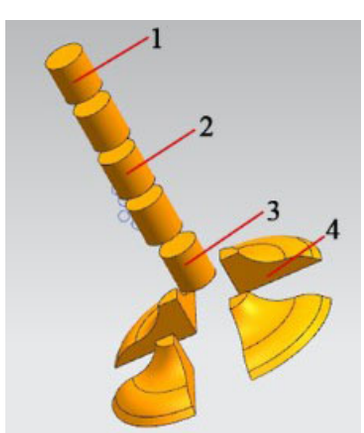

Fig.4 Cutting diagram of a specimen

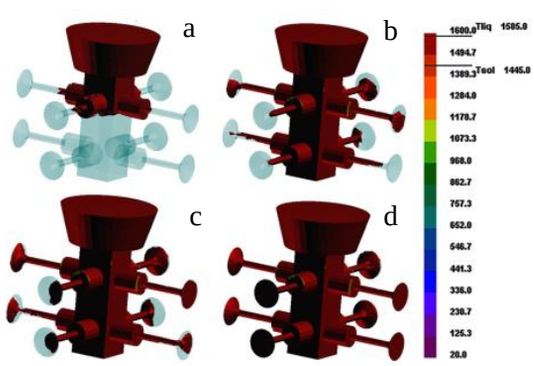

Fig.5 Typical simulation schematics of filling process for valves at different filling time: (a) t=2.47 s, (b) t=2.83 s, (c) t=3.22 s, and (d) t=3.89 s

cavity is fully filled. Fig.6 shows the potential porosity locations of casting simulation results of exhaust valves. Based on the finding in Fig.6, it is indicated that visible shrinkage porosity of all the exhaust valves is distributed along the axis of valves, especially in the neck position. The defects are mainly caused by the filling order and temperature effects. So, the complete structure without defects can be obtained by the available process parameter and gating system to ensure the directional solidification and adequate feeding of melt.

Fig.7 shows images of the solidified valves with or without the ceramic shell mold. As shown in Fig.7b, the sound exhaust valves in the bottom layer can be produced. The main reason is that the thickness of the alloy solidification shell is much larger. Besides, the temperature of the preheated shell mold is lower. When the molten alloy is poured into the center

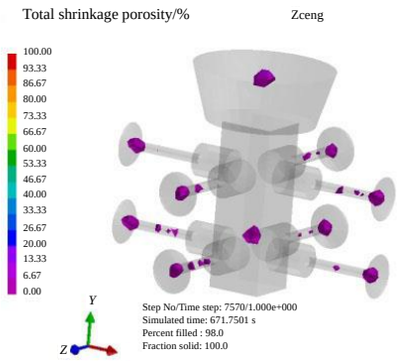

Fig.6 Shrinkage porosity location of simulation

Fig.7 Valve casting with (a) and without (b) the ceramic shell mold

of the mold, the alloy in the running and gating system will also rotate under the centrifugal force. The alloys reach the inner shell and start to solidify, which causes insufficient melt alloy to shape valves. The actual mold filling results are exactly the opposites of the simulation results, as shown in Fig.5. The possible reason is that for the bottom layer, four valves on the "tree-type" shell are filled fully at the same time in initial filling due to the gravity effect. The valve cavities are filled randomly in different layers as the alloy filling goes on. The exhaust valves in the upper layer are filled later than those in the lower layer, together with the insufficient melt alloy. Fig. 8 shows the typical defects of actual castings, such as misrun and shrinkage porosity. As shown in Fig.8, shrinkage porosity location in casting is agreed with the simulation results. The formation of misrun defects at the edge of the exhaust valve's head is related to the filling process, like pouring temperature

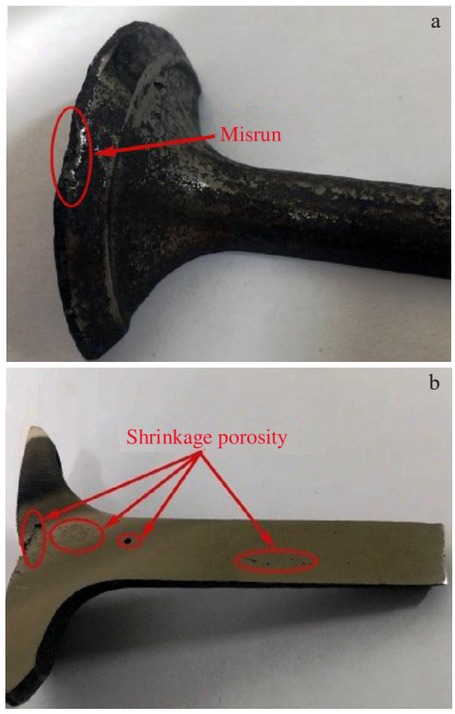

Fig.8 Macroscopic defects in actual castings: (a) misrun and (b) shrinkage porosity

or preheating temperature of shell mold. When the melted alloy is poured through the stem into the head, the melt-filled front parts fill half of the head, while leaving the other half-unfilled. As the filling of the valve head goes on, the gas volume is accumulated and surrounded in the center axis of the neck, forming the porosity in the subsequent solidification.

2.2 Variation of viscosity for inner layer slurry in making shell mold

The quality of the inner surface for the shell mold is the key factor influencing the surface quality of precision castings. Suitable inner layer slurry, the premise for making shell mold, requires proper viscosity and good fluidity. It can not only reproduce the casting model accurately but also form a uniform thickness for the inner layer of the shell. The powder/liquid ratio and mixing time are the key factors affecting the performance of inner layer slurry in making shell mold. The variation of viscosity for inner layer slurry is evaluated by adjusting the powder/liquid ratio and mixing time. During the experiments, the powder/liquid ratio is set as 1:1, 1.5:1 and 1.8:1 to make three kinds of inner layer slurry. Then, the variation of viscosity for three types of slurry is investigated at different mixing time. Fig. 9 shows the relationship between viscosity and mixing time for different powder/liquid ratios of inner layer slurry.

From Fig.9, it is revealed that the viscosity of inner layer slurry increases as the powder/liquid ratio increases. Among them, the inner layer slurry with a powder/liquid ratio of 1.8:1 has the most considerable viscosity. The possible reason is

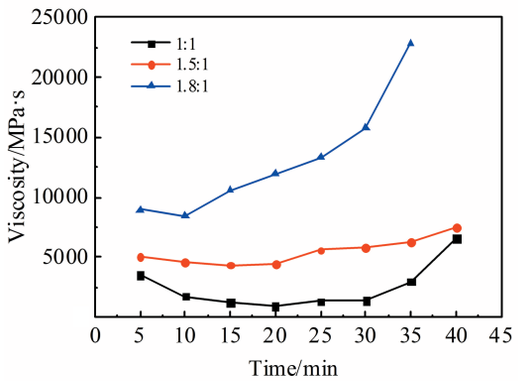

Fig.9 Relationship between viscosity and mixing time for different powder/liquid ratios of inner layer slurry

that there are many kinds of bonds inside the slurry. The cubic structure grids are formed by the powders and zirconia sol, which are connected under the action of these bonding forces. The content of the solid phase in the slurry is increased as the powder/liquid ratio gets bigger. With higher solid content in the slurry, the interaction among particles is more reliable due to more internal nodes among them per unit volume in the system. So, the higher the powder/liquid ratio, the higher the slurry viscosity. The viscosity of the three kinds of slurry decreases gradually in the first 10 min of mixing and then increases gradually with the extension of mixing time. The possible reason is that the interaction of slurry cannot be immediately achieved at the first stage of mixing. This connection gradually forms with the rearrangement of cubic structure grids, and the viscosity tends to decline in this process. After mixing for some time, the strong grid structure is formed in the slurry because the interaction among particles is strengthened. As the strength of the grid structure is increased, the viscosity of slurry has an upward tendency. Based on the experiment, the powder/liquid ratio of 1.5:1 and mixing time of 30 min are identified as the proper process for inner layer slurry in making shell mold in this research.

2.3 Evaluation of microstructures for castings

To evaluate the interfacial reaction between casting and inner shell mold, the X-ray diffraction analysis of valve castings is performed. Fig. 10 shows the XRD patterns of specimens. As described above in Fig. 4, the samples shown in Fig.8 are cut from the valve casting. Based on Fig.10, it is revealed that the γ-TiAl is the primary phase with a small amount of α_2-Ti_3Al. Besides, no other phases are detected. It can be indicated that there is no apparent interfacial reaction in the whole process. In other words, the method developed for making shell mold is appropriate in this study.

Fig. 11 shows the typical microstructures of the specimens. It is revealed that there is no significant change among the specimens at different positions. All the specimens have a

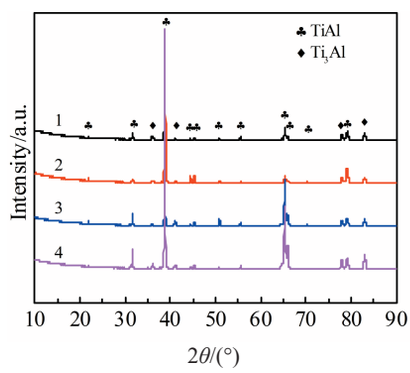

Fig.10 XRD patterns of the specimens for valve castings

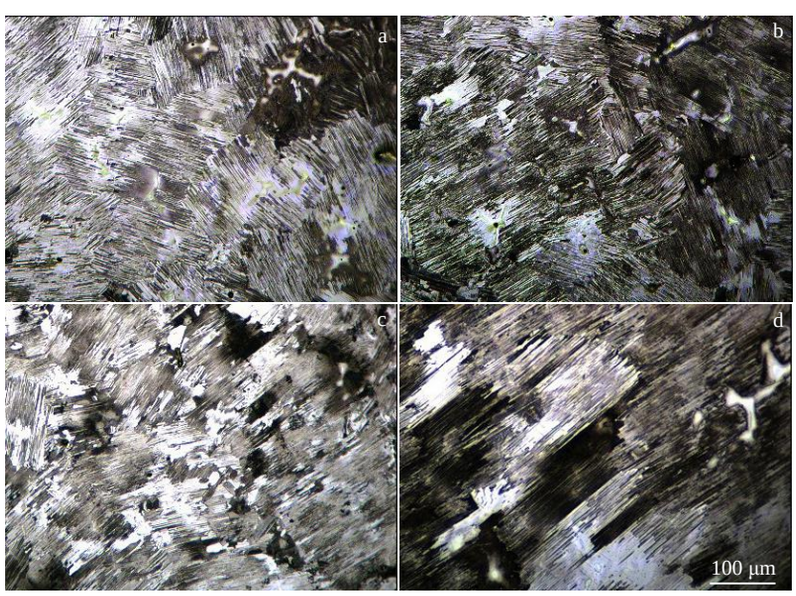

Fig.11 OM micrographs of the four specimens: (a) specimen 1, (b) specimen 2, (c) specimen 3, and (d) specimen 4

regular full lamellar structure for TiAl alloys. The average grain size of samples is 185, 285, 220, and 305 μm. The four specimens represent different cooling rates for alloy solidification. In the case of this work, the centrifugal rotation increases the equivalent interfacial heat-transfer coefficient between molten and shell, which results in the fast cooling rate during solidification that is the predominant factor influencing the grain size.

3 Conclusions

1) The shell mold filling process and solidification of TiAl exhaust valves by centrifugal investment casting are simulated and produced successfully. A "tree-type" of gating system is designed and adopted to assemble in the experiment.

2) The simulation results show that the full filling time is about 3.8 s, and the shrinkage porosities are distributed along the central line of the exhaust valve, especially in the neck position.

3) In actual castings, the macroscopic casting defects such as misrun, shrinkage porosity, and entrapped porosity are observed, showing the right consistency with the simulation results. The powder/liquid ratio of 1.5:1 and mixing time of 30 min are chosen as the proper process for inner layer slurry in the making shell mold process.

4) There are no visible interfacial reactions between casting and shell mold. The lamellar structure is observed in the as-cast exhaust valves, with a grain size of 185~305 μm. It is possible for the mass production of high-Nb TiAl exhaust valves by the centrifugal investment casting process.

References

1 Wu Shiping, Guo Jingjie, Su Yangqing *et al*. *International Journal of Cast Metals Research*[J], 2003, 15(3): 137

2 Humphreys N J, McBride D, Shevchenko D M *et al*. *Applied Mathematical Modeling*[J], 2013, 37(14-15): 7633

3 LoriaEdward A. *Intermetallics*[J], 2000, 8(9-11): 1339

4 Wu Xinhua. *Intermetallics*[J], 2006, 14(10-11): 1114

5 Chen G L, Wang J G, Ni X D *et al*. *Intermetallics*[J], 2005, 13(3-4): 329

6 Lin J P, Zhao L L, Li G Y *et al*. *Intermetallics*[J], 2011, 19 (2): 131

7 Sung S Y, Kim Y J. *Materials Science and Engineering A*[J], 2005, 405(1-2): 173

8 BarbosaJoaquim, Silva Ribeiro C, Caetano Monteiro A. *Intermetallics*[J], 2007, 15(7): 945

9 Jovanović M T, Dimčić B, Bobić I *et al*. *Journal of Materials Processing Technology*[J], 2005, 167(1): 14

10 Bartels Arno, Kestler Heinrich, Clemens Helmut. *Materials Science and Engineering A*[J], 2002, 329-331: 153

11 Li Changyun, Wang Haiyan, Wu Shiping *et al*. *Rare Metal Materials and Engineering*[J], 2010, 39(3): 388

Ti-47Al-6Nb基排气阀的熔模离心铸造工艺

许荣福，李常厚，徐　勇，张东明，时月亚

(山东建筑大学 材料科学与工程学院，山东 济南 250101)

摘　要：研究了高Nb钛铝基排气阀铸件的熔模离心铸造工艺，排气阀铸件的化学成分确定为Ti-47Al-6Nb （at%），所用型壳材料为锆砂。为了与模拟充型结果进行比较和验证浇注工艺，进行了排气阀的离心铸造模壳充型实验。模拟结果表明：模壳充型时间约为3.8 s，铸件缺陷沿排气阀中心线分布，特别是在颈部位置处；经过实验验证，模拟结果和实验结果吻合度较好。实验过程中，模壳挂涂所需内层浆料的适宜工艺确定为粉液比是1.5:1，搅拌时间30 min。通过对排气阀铸件表面进行XRD测试，结果表明铸型与壳型之间没有明显的界面反应；排气阀铸件的金相组织为典型的层状结构，晶粒尺寸在185~300 μm之间。

关键词：排气阀；数值模拟；宏观缺陷；微观组织

作者简介：许荣福，男，1984年生，博士，讲师，山东建筑大学材料科学与工程学院，山东 济南 250101，电话：0531-86367286，E-mail：13559@sdjzu.edu.cn